

Synthesis and DFT investigation of new bismuth-containing MAX phases

Horlait, Denis , Middleburgh, Simon C. , Chroneos, A. and Lee, William E.

Published PDF deposited in [Curve](#) January 2016

Original citation:

Horlait, Denis , Middleburgh, Simon C. , Chroneos, A. and Lee, William E. (2016) Synthesis and DFT investigation of new bismuth-containing MAX phases. Scientific Reports, volume 6 (Article number: 18829). DOI: 10.1038/srep18829

<http://dx.doi.org/10.1038/srep18829>

Nature Publishing Group

This work is licensed under a Creative Commons Attribution 4.0 International License.

Copyright © and Moral Rights are retained by the author(s) and/ or other copyright owners. A copy can be downloaded for personal non-commercial research or study, without prior permission or charge. This item cannot be reproduced or quoted extensively from without first obtaining permission in writing from the copyright holder(s). The content must not be changed in any way or sold commercially in any format or medium without the formal permission of the copyright holders.

CURVE is the Institutional Repository for Coventry University

<http://curve.coventry.ac.uk/open>

SCIENTIFIC REPORTS

OPEN

Synthesis and DFT investigation of new bismuth-containing MAX phases

Denis Horlait¹, Simon C. Middleburgh^{2,3}, Alexander Chroneos^{1,4} & William E. Lee¹

Received: 07 September 2015

Accepted: 17 November 2015

Published: 07 January 2016

The $M_{n+1}AX_n$ phases (M = early transition metal; A = group A element and X = C and N) are materials exhibiting many important metallic and ceramic properties. In the present study powder processing experiments and density functional theory calculations are employed in parallel to examine formation of $Zr_2(Al_{1-x}Bi_x)C$ ($0 \leq x \leq 1$). Here we show that $Zr_2(Al_{1-x}Bi_x)C$, and particularly with $x \approx 0.58$, can be formed from powders even though the end members Zr_2BiC and Zr_2AlC seemingly cannot. This represents a significant extension of the MAX phase family, as this is the first report of a bismuth-based MAX phase.

The MAX phases are a family of ternary carbides and nitrides. To be designated as a MAX phase, a compound should crystallize with the hexagonal $P6_3/mmc$ structure in the general formula $M_{n+1}AX_n$ with n being an integer, M being an early transition metal, A being a group 13–16 element and X being C and/or N¹. More than half of known MAX phases were first synthesized in the 1960s by Nowotny *et al.*² They were little studied for more than two decades until Barsoum and El-Raghy reported in 1996 the remarkable properties of Ti_3SiC_2 ³ and further demonstrated these properties were shared by the other MAX phases^{4,5}. Indeed, due to their structure consisting of the stacking of n “ceramic” layer(s) of MX interleaved by an A “metallic” plane, MAX phases are characterized by a combination of both ceramic and metallic behavior. Like most metals and alloys, they possess high thermal shock resistance, have a good machinability, and high thermal and electrical conductivities while like most ceramics they have high decomposition or melting temperature and high elastic stiffness¹. Furthermore, MAX phases are also of interest as precursors for MXenes ($M_{n+1}X_n$ two-dimensional nanosheets with properties analogues to graphene) currently only synthesizable by selective chemical etching of mostly Al-based MAX phases^{6,7}.

From 1996 to 2004, intensive research expanded the MAX phase family to more than 60 compositions that included 9 different “M” elements, 12 different “A” elements and n values of 1, 2, and 3^{1,8,9}. Since then, new discoveries reported have mainly focused on MAX phases with higher n values and on solid solutions^{9–11}, *i.e.* partial substitution of the M, A or X elements, hence broadening to a quasi-infinite number of possible combinations. In 2014, Naguib *et al.*¹⁰ listed 68 quaternary MAX phases compositions already reported. Quaternary MAX phases also offer the possibility of including new elements that do not form alone a bulk ternary MAX phase, such as Mn recently incorporated in $(Cr_{1-x}Mn_x)_2GaC$ ($0 \leq x \leq 0.3$) by Mockute *et al.*¹²

The crystal structure of the M_2AX phases (or 211 MAX phases) is given in Fig. 1. For the M_2AX phase the structure can be described as a highly symmetric hexagonal unit cell that contains atomic layers of the constituent elements stacked along the c direction. Two M layers enclose an X layer of atoms forming an M_2X slab with a local fcc-type stacking sequence. Atomic layers of A separate the M_2X slabs. Local stacking around the A layer has an hcp pattern and thus the A layer forms a mirror plane in the crystal. The crystal structure can be defined by the a and c lattice vectors and the interplanar separation between the M and X atomic layers (d_{MX}).

A potentially significant application of MAX phases is their use by the nuclear industry. Ion and neutron irradiations studies performed since 2009^{13,14}, determined the good resistance (low swelling, limited decomposition or amorphisation) of MAX phase carbides and notably of Ti_3SiC_2 . These properties make MAX phases candidate materials *e.g.* in the capacity of protective coatings for zirconium alloy nuclear fuel cladding. As tragically reminded by the recent events of Fukushima, in the case of a Loss-of-Cooling Accident (LOCA) and the impossibility to

¹Department of Materials and Centre for Nuclear Engineering, Imperial College London, London SW7 2BP, United Kingdom. ²IME, Australian Nuclear Science and Technology Organisation, Lucas Heights, New South Wales, Australia. ³Westinghouse Electric Sweden, SE-721 63 Västerås, Sweden. ⁴Faculty of Engineering, Environment and Computing, Coventry University, Priory Street, Coventry CV1 5FB, United Kingdom. Correspondence and requests for materials should be addressed to D.H. (email: denishorlait@hotmail.com) or S.C.M. (email: middleesc@westinghouse.com) or A.C. (email: alexander.chroneos@imperial.ac.uk)

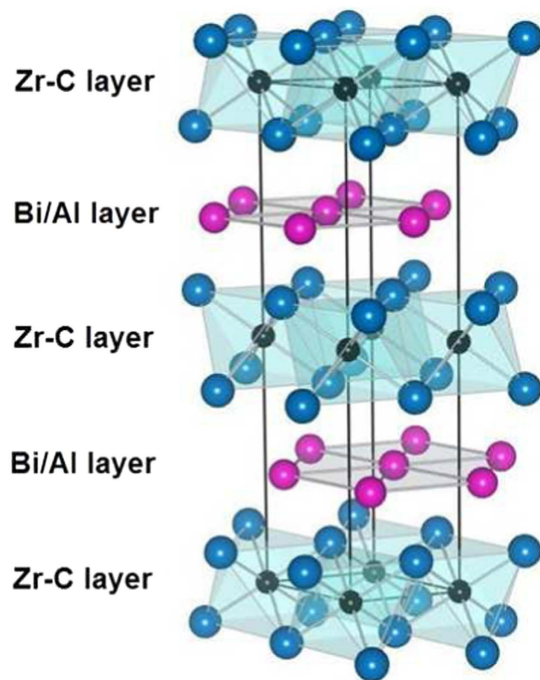


Figure 1. Representation of the $P6_3/mmc$ crystalline structure of the 211 MAX phases. Blue atoms: Zr; black atoms: C and pink atoms: Bi or Al. The unit cell is delimited by the plain black lines.

temper the reactor temperature, Zr clads can react over about 1200 °C with residual steam to catalytically produce H_2 , eventually leading to release of nuclear fuel in the reactor and to dramatic explosions. A way to avoid or at least postpone this catalytic reaction is via the protection of the nuclear fuel clad against high-temperature oxidation. Among the MAX phases, Zr_2AlC would be advantageous as 1) Zr has a very high neutron transparency and is the main constituent of the substrate clad, 2) Al by its presence on the A metallic planes is likely to readily diffuse out to form an alumina protective layer appropriate for high temperature oxidation protection analogously to what is achieved for Ti_2AlC ¹ and 3) C, as opposed to ^{14}N does not lead to problematic activation products. Nevertheless, to our knowledge, there are no reports on the synthesis and thereby on the actual existence of Zr_2AlC . It can be argued that other non-MAX phase ternary layered carbides such as $Zr_2Al_3C_4$ could be suitable¹⁵, however the reported oxidation resistance of these carbides is insufficient¹⁶.

One possible way then to obtain a material having similar properties as those anticipated for Zr_2AlC is to partially substitute one of the constituting elements by another one stabilizing the structure. As the number of possibilities to test is experimentally constraining, an informed pre-selection of compositions to investigate is necessary. In this sense and in respect to our targeted nuclear application, elements with high neutron cross-section (i.e. Hf, Ta, Cd and In notably) have to be avoided. Then, density functional theory (DFT) calculations can provide important insights into the material properties and phase stability of the candidate $M_{n+1}AX_n$ phases that can be complementary to experimental studies^{17–21}. Notably, for some of the $M_{n+1}AX_n$ phases there is little empirical information as experiments are hindered by the difficulty of producing single phase samples^{22,23}. Considering phase stability, previous DFT studies^{24–26} have correctly predicted the stability (or not) of $M_{n+1}AX_n$ phases with respect to their competing phases.

In the present study DFT is employed to investigate the phase stability and structure of $Zr_2(Al_{1-x}Bi_x)C$ ($0 \leq x \leq 1$) while attempts were performed in parallel to form $Zr_2(Al_{1-x}Bi_x)C$ by powder processing.

Results and Discussion

Syntheses and characterizations. Heat treatments at 1300 °C and 1450 °C were initially chosen considering the conditions reported for the synthesis of other Zr_2AC MAX phase^{4,27–30} to try producing Zr_2BiC , $Zr_2(Al_{0.50}Bi_{0.50})C$ and Zr_2AlC . On the basis of initial results, a 1150 °C treatment was also tried. Phase determinations from X-ray diffraction (XRD) of all attempted syntheses are summarized in Table 1. Neither Zr_2AlC nor Zr_2BiC were obtained, whatever the temperature of reaction. This is consistent with the absence of reports of Zr_2AlC and Zr_2BiC syntheses, although 5 other Zr_2AC MAX phases can be formed in similar experimental conditions ($A = S, Sn, In, Tl$ or Pb)^{4,27–31}. This also confirms that Zr_2AlC and Zr_2BiC are not (meta-)stable and/or are less stable than the combination of $ZrC + ZrAl_2$ or $ZrAl_3$ and $ZrC + Bi +$ one unknown phase respectively obtained instead (Table 1).

More importantly, XRD determined that the attempt to synthesize $Zr_2(Al_{0.50}Bi_{0.50})C$ at 1300 °C was partially successful as a MAX phase was formed along with ZrC and $ZrAl_2$ (Fig. 2). During Energy Dispersive X-ray spectrometry (EDX) characterization, point analysis of over 10 independent MAX phase grains gave elemental ratio of $(Al + Bi)/(Zr + Al + Bi)$ of 0.33(3), hence agreeing perfectly with a 211 MAX phase, and a $Bi/(Al + Bi)$ ratio of

Targeted compound	Reaction temperature	Observed phases
Zr ₂ AlC	1450 °C	ZrC + ZrAl ₂
Zr ₂ (Al _{0.50} Bi _{0.50})C		ZrC + ZrAl ₂ + Unknown
Zr ₂ BiC		ZrC + Bi + Unknown
Zr ₂ AlC	1300 °C	ZrC + ZrAl ₂
Zr ₂ (Al _{0.50} Bi _{0.50})C		Zr ₂ (Al _{0.42} Bi _{0.58})C + ZrC + ZrAl ₂ + Unknown
Zr ₂ BiC		ZrC + Bi + Unknown
Zr ₂ AlC	1150 °C	ZrC + ZrAl ₃
Zr ₂ (Al _{0.50} Bi _{0.50})C		Zr ₂ (Al _{0.42} Bi _{0.58})C + ZrC + Zr ₃ Al ₄
Zr ₂ (Al _{0.41} Bi _{0.59})C		Zr ₂ (Al _{0.42} Bi _{0.58})C + ZrC + Zr ₃ Al ₄
Zr ₂ BiC		ZrC + Bi + Unknown

Table 1. Summary of synthesis results.

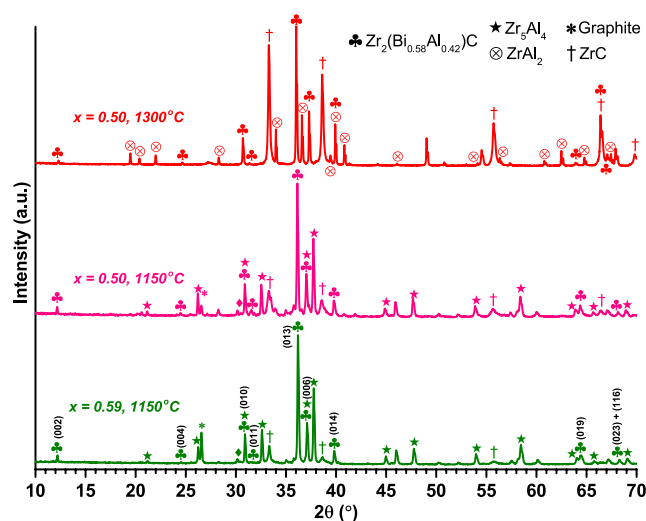


Figure 2. X-ray diffractograms of ZrH₂ + Bi + Al + C powder mixes reacted for 10 h at 1300 or 1150 °C for Bi/(Al + Bi) ratios of 0.50 and 0.59.

0.58, with a dispersion of only ± 0.02 , indicating the formation of Zr₂(Al_{0.42}Bi_{0.58})C. Note that the deviation from the targeted stoichiometry 1:1 Al:Bi is in agreement with the presence of ZrAl₂ as a secondary phase, accommodating excess Al. Furthermore, Spark Plasma Sintering (SPS) was realized on the 1300 °C Zr₂(Al_{0.50}Bi_{0.50})C sample at the same temperature at 35 MPa for 10 minutes. Unexpectedly, the MAX phase content in the resulting densified ceramic sample dropped almost to zero with ZrC and ZrAl₂ XRD patterns rising concomitantly. As it has never been reported that such pressure can decompose a MAX phase, it is more likely the decomposition temperature of the Zr₂(Al_{0.42}Bi_{0.58})C MAX phase lies somewhere around 1300 °C and is more advanced in SPS due to a temperature overshoot at the end of the heating ramp and/or because the vacuum helps Bi evaporating out of the system during the decomposition process. This concurs with Barsoum *et al.*⁴ and El-Raghy *et al.*²⁸ works who found, respectively for Zr₂SnC and Zr₂PbC, that the decomposition temperature of such MAX phase is around 1300 °C.

From these initial findings, a lower temperature of synthesis was chosen, 1150 °C, and was employed to attempt to synthesize the same Zr₂(Al_{1-x}Bi_x)C compounds with $x = 0, 0.50$ and 1. As it was anticipated the Zr₂(Al_{0.42}Bi_{0.58})C compound obtained at 1300 °C could be the result of a particular structural stabilization process, a powder mix targeting Zr₂(Al_{0.41}Bi_{0.59})C was also prepared and fired at 1150 °C (x value of 0.59 was selected instead of 0.58 to comply with the ratio $19/32 \approx 0.59$ which was the closest ratio achievable in the DFT calculations). Here again Zr₂BiC and Zr₂AlC syntheses were unsuccessful, whilst for mixed compositions a single MAX phase was produced as the main phase as reported in Fig. 2. Figure 2 reveals that the relative ZrC content decreases with decreasing synthesis temperature as well as when targeting Zr₂(Al_{0.41}Bi_{0.59})C instead of Zr₂(Al_{0.50}Bi_{0.50})C. It is interesting to note that for all three syntheses that lead to the formation of a MAX phase, EDX characterization always gave an average Bi/(Al + Bi) ratio of 0.58 (± 0.02 to 0.04 scatter). This is indirectly confirmed by comparing the unit cell parameters determined by XRD data refinement as the $x = 0.50$ and $x = 0.59$ syntheses at 1150 °C have very close unit cell parameters and corresponding volumes ($a = 3.335(5)$ Å, $c = 14.51(2)$ Å, $V = 139.8(4)$ Å³ and $a = 3.344(5)$ Å, $c = 14.51(2)$ Å, $V = 140.6(5)$ Å³, respectively).

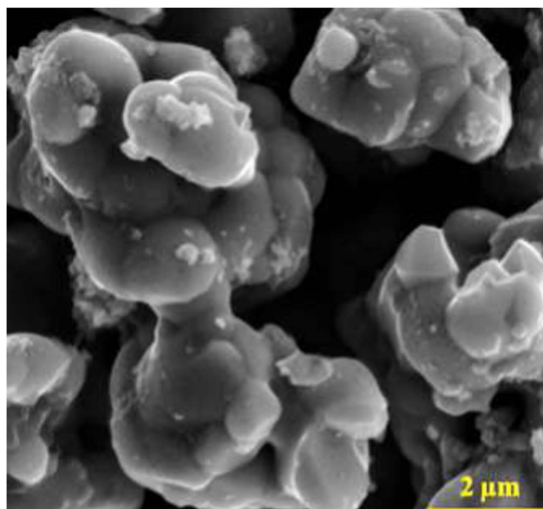


Figure 3. SEM image (secondary electron imaging mode) of $Zr_2(Al_{0.42}Bi_{0.58})C$ powder ($Zr_2(Al_{0.41}Bi_{0.59})C$ synthesis attempt at $1150^\circ C$).

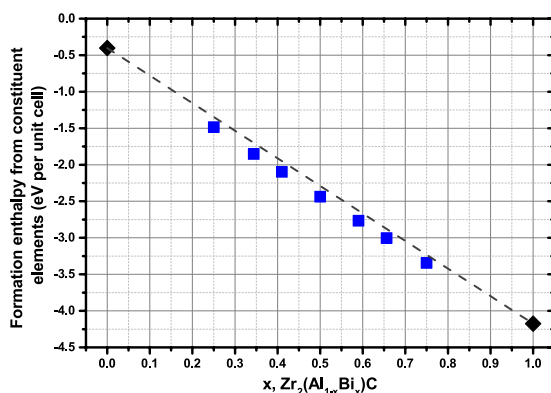


Figure 4. Variation in formation enthalpy of $Zr_2(Al_{1-x}Bi_x)C$ per unit as a function of Bi content. The gray dashed line represents the proportional variation between the two end-members.

Figure 3 is a representative SEM image of $Zr_2(Al_{0.42}Bi_{0.58})C$ grains (composition checked by EDX on this precise location). The powders consist of 2 to 10 microns agglomerates of stacked rounded platelets. Interestingly, this microstructure and grain size does not differ as a function of targeted composition ($Zr_2(Al_{0.41}Bi_{0.59})C$ vs. $Zr_2(Al_{0.50}Bi_{0.50})C$) or of temperature (1150 vs. $1300^\circ C$). SEM imaging of large areas ($\approx 10,000 \mu m^2$) of synthesized powders reveals that such agglomerates represent a vast majority of the volume (around 90 vol.% for $1150^\circ C$ $Zr_2(Al_{0.41}Bi_{0.59})C$), which suggests the samples consist mainly of $Zr_2(Al_{0.42}Bi_{0.58})C$. Again the synthesis temperature was found to have little effect on sample phase composition and the only actual difference, revealed by XRD (Fig. 2) and SEM/EDX between 1150 and $1300^\circ C$ is the nature and relative ratios of the detected secondary phases (ZrC , Zr_5Al_4 , $ZrAl_2$).

Density functional theory calculations. Nine stoichiometries were considered for DFT calculations: $x = Bi/(Al + Bi) = 0, 0.25, 0.34, 0.41, 0.50, 0.59, 0.66, 0.75$ and 1 . The formation enthalpy of all nine stoichiometries was calculated from the constituent elements, as described in the methodology. The formation enthalpy of the Zr_2AlC compound was calculated to be $-0.40 eV$ and the formation enthalpy of the Zr_2BiC was calculated to be $-4.17 eV$. Both are negative indicating that they are more stable compared to their constituent compounds ($Zr + C + Al$ or Bi). The formation enthalpies for all stoichiometries are reported in Fig. 4. For $Zr_2(Al_{1-x}Bi_x)C$ solid solutions, the formation enthalpies are close but however all slightly inferior to the values expected considering a proportionality between Zr_2BiC and Zr_2AlC end-members values.

The mixing enthalpies of the compounds (mixed from a stoichiometric combination of Zr_2AlC and Zr_2BiC) are now discussed. As can be ascertained from Fig. 5, all mixing enthalpies of the considered stoichiometries are negative. Therefore DFT calculation predicts that quaternary $Zr_2(Al_{1-x}Bi_x)C$ will be formed preferably rather than a mixture of Zr_2AlC and Zr_2BiC , at least for the considered x range ($0.25 \leq x \leq 0.75$). This is in agreement with our experimental results finding formation of $Zr_2(Al_{0.42}Bi_{0.58})C$ over $Zr_2AlC + Zr_2BiC$.

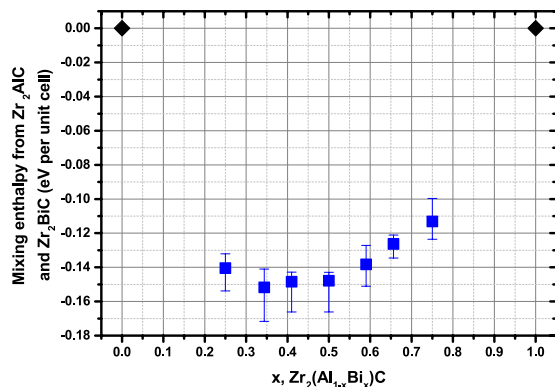


Figure 5. Variation in mixing enthalpy of $Zr_2(Al_{1-x}Bi_x)C$ per unit cell as a function of Bi content. Each error bar give the minimum and maximum values determined out of 10 independent simulation box while each square dot gives the average value.

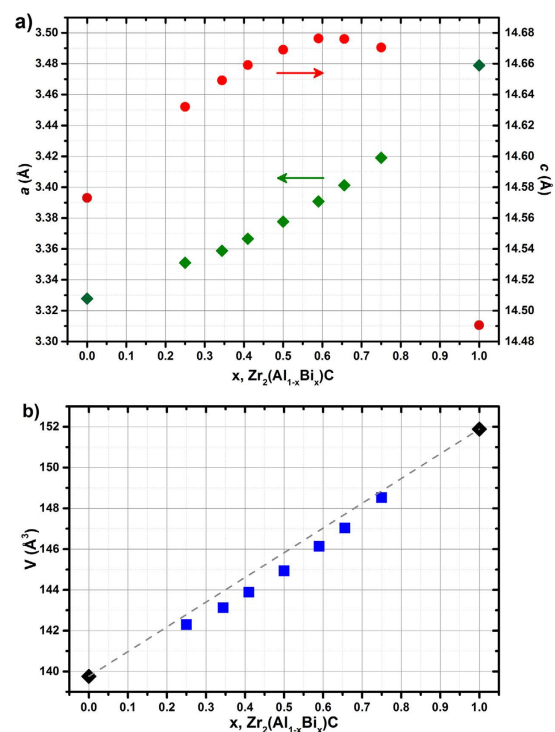


Figure 6. Variation of (a) the a and c lattice parameters and of (b) the corresponding volume with the Bi content in $Zr_2(Al_{1-x}Bi_x)C$. The gray dashed line in (b) represents the proportional variation of volume between the two end-members.

Another relevant piece of information from DFT calculations is that amongst each series of ten $Zr_2(Al_{1-x}Bi_x)C$ simulation boxes, the Al and Bi starting repartitions are random but different. In spite of this, there is no outlier and the dispersion of obtained results is low (this is evidenced by the low dispersion obtained in Fig. 5, $\sim \pm 0.01$ eV per unit cell). This implies Al and Bi repartition do not seem to have any importance on the structure stability and therefore suggests that the relative higher stability of $Zr_2(Al_{1-x}Bi_x)C$ with $0.25 \leq x \leq 0.75$ over the other compositions is presumably not experimentally achieved through an ordering of the two A elements.

The mixing enthalpy values are close one to another and Fig. 5 therefore does not help in understanding why the $x = 0.58$ composition appears to form experimentally over other stoichiometries. Further analysis of the data produced by DFT calculations may however give some hints on the origin of the enhanced stability of $Zr_2(Al_{0.42}Bi_{0.58})C$ and conversely explain the non-stability of the end-members. The following paragraphs and Figures therefore aim to present the evolution of some relevant features observed in the simulations.

Figure 6a presents the evolution of unit cell parameters determined by the *ab initio* calculations. The a lattice parameter monotonically increases as a function of x (from Zr_2AlC to Zr_2BiC , a increases by 4.5%). In other

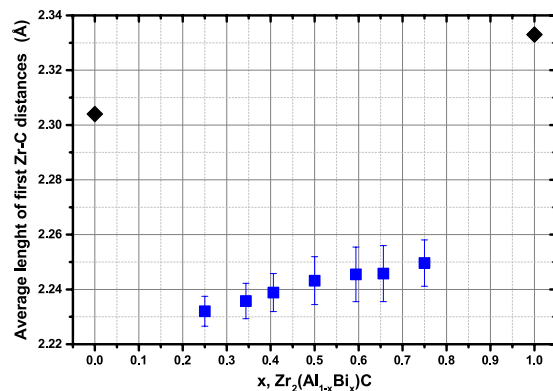


Figure 7. Variation of the average first Zr-C distance with the Bi content in $Zr_2(Al_{1-x}Bi_x)C$ determined from the DFT calculations. The error bars correspond to the standard deviation of all measured distances.

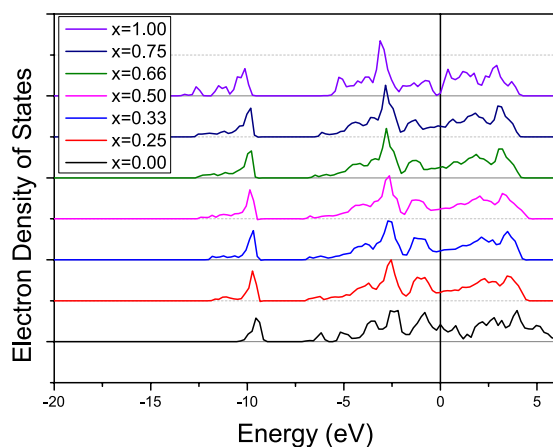


Figure 8. Density of states of $Zr_2(Al_{1-x}Bi_x)C$. The 0 eV value corresponds to the Fermi level.

words, the C-C (first neighbors) distances and therefore the (0001) plane of the unit cell (Fig. 1) are proportionally expanding with Bi incorporation. The c parameter variation is quite different as the maximum c lattice parameter is obtained for $x = 0.59$, i.e. the experimentally most stable composition ($Zr_2(Al_{0.42}Bi_{0.58})C$), then unexpectedly drops between $x = 0.75$ and 1 for a reason that is explained later in this paper. The difference between the maximum and minimum c values (at $x = 0.59$ and $x = 1$ respectively) is of 1.0%, therefore 4.5 times less than a maximum variation, meaning that changes in the A element size and nature mainly impact the a lattice parameter. Figure 6b shows that the unit cell volume increases with Bi incorporation, as expected by the larger size of Bi compare to Al. The cell volume increases proportionally to x and follows rather well Vegard's law (i.e. the proportional variation between the two end-members).

In Fig. 7 the evolution of first neighbors Zr-C distances are reported. An important decrease is first seen between Zr_2AlC and $Zr_2(Al_{0.75}Bi_{0.25})C$. It is expected by the incorporation of larger Bi atoms (Bi metallic radius is 1.70 Å, Al is 1.429 Å) which expands the A layer in the structure therefore compressing the Zr_2C blocks. For the quaternary compositions it is seen that the Zr-C distances are increasing by 0.8% between $x = 0.25$ and $x = 0.75$. Therefore the increase in incorporation rate of larger Bi into the structure is found by DFT calculations to be accompanied by a relaxation of the Zr-C bonds. At the same time the c lattice parameter is calculated to be little impacted by Al substitution by Bi, while a is greatly increased (+0.26% and +2.0% in the same interval for a and c , respectively). It is thus concluded that for the treated quaternary compositions, the increase in incorporation rate of Bi is accommodated through a compression of the Zr-C layers along the c -axis itself mostly relaxed by an expansion along the (0001) plane.

Figure 7 also reveals the Zr-C distances for Zr_2BiC are far greater than those of the quaternaries (+4%). In view of the lattice dimensions evolution reported in Fig. 6, this result was quite unexpected. Such steep variation of property between $Zr_2(Al_{0.25}Bi_{0.75})C$ and Zr_2BiC was also found when drawing up and comparing the density of states (DOS) (Fig. 8). While the DOS of the quaternary compositions are similar to each other and are typical of those of other 211 MAX phases^{1,32}, that of Zr_2BiC has little or no electron density at the Fermi level, creating a pseudogap (Fig. 8). This implies that the bonding nature between Bi and Zr is abnormally more covalent and less metallic than in most of the other MAX phases, including the quaternary systems for which somehow the replacement of $\frac{1}{4}$ of the Bi by Al prevents most if not all of such high covalence of the Zr-A bond. As a consequence of the enhanced Zr-Bi covalence in Zr_2BiC , the Zr-Bi bond shrinks and so does the structure along the c -axis, retrospectively

explaining the drop in c observed in Fig. 6a between $x = 0.75$ and 1. A similar set of features (DOS and c lattice parameter) has been previously encountered and reported by Barsoum³² for Ti_2SC and given the relatively low c -parameter of Zr_2SC , the latter should be part of this small group of outliers. Even if this atypical most-stable state found by the DFT calculations does not explain why Zr_2BiC appears experimentally non-synthesizable contrary to $Zr_2(Al_{0.42}Bi_{0.58})C$ – Ti_2SC is a living proof that a peculiar bonding structure can be (meta-)stable – it however presumably proves that the better stability of the quaternary compositions compared to Zr_2BiC arises from Al presence precluding Bi to lose its metallic characteristic.

Discussion and summary. At this point the question is “Why can we produce a quaternary $Zr_2(Al_{1-x}Bi_x)C$ while we seemingly cannot produce any of the two ternary end members?” And following this, we can also wonder “What is so special about $Zr_2(Al_{0.42}Bi_{0.58})C$ composition so that this later forms over other stoichiometries?” With the results available, this second question can hardly be answered. Aside from the fact that DFT calculations along a compositional range are rarely finding exactly the same threshold tipping values as the ones found in real experiments, none of the DFT-derived results clearly highlight a particular behavior for a certain x value in the $0.25 \leq x \leq 0.75$ range. The only notable point is that the lowly varying c lattice parameter is maximum for $Zr_2(Al_{0.41}Bi_{0.59})C$ suggesting the experimental selection of the $x = 0.58$ stoichiometry may be driven by steric considerations.

About the apparent non-stability of Zr_2AlC and Zr_2BiC while $Zr_2(Al_{0.41}Bi_{0.59})C$ is stable, this is actually a more wide open question, since despite many efforts^{1,33}, we still lack a comprehensive picture of what is driving ternary and *a fortiori* quaternary MAX phases’ stability. That is, advanced DFT calculations can predict fairly well whether a MAX phase is stable or not and whether it will form over competing phases or not if the formation enthalpies of these competing phases are also calculated^{1,23–25,33}. DFT and other experimental data comparison also pointed out c/a ratios, valence electron concentration¹ and shear modulus/bulk modulus ratio³³ are likely to be key parameters regarding stability but however at the current stage, all these DFT related works have not been able to elicit a simple and universal predicting rule from constituting elements characteristics such as *e.g.* ionic radius or c/a ratios. Once again a presumable main part of the problem should be that a MAX phase existence does not only depend on its own structural stability but also on that of all possible competing phases^{24,25}.

In the present case, the simplest possible answer to the first question obviously is that Zr_2AlC and Zr_2BiC are structurally less stable than the combination of phases experimentally obtained (Table 1). Nonetheless it is also likely that the experimental formation of a MAX phase can be precluded because of a disadvantageous combination of onset temperatures of formation (T_f) and of decomposition (T_d) and potentially of the associated kinetics (k_f and k_d) of the two reactions. As discussed before in this paper, T_f and T_d are often close for Zr_2AC MAX phases^{4,28}. It is then possible we do not obtain either Zr_2AlC or Zr_2BiC because $T_d \ll T_f$ or because $T_d \approx T_f$ but for the tested temperatures $k_d \gg k_f$. Whatever the reason for the experimental absence of Zr_2AlC and Zr_2BiC although nothing from DFT works directly suggests a non-stability^{34–37}, the quaternary $Zr_2(Al_{0.42}Bi_{0.58})C$ somehow produces an enhanced structural stability, which results in rendering the formation of the MAX phase more energetically favorable than competing phases and/or in favorably changing the T and k above-defined values, so that formation takes over decomposition. As it can be simply seen with a periodic table and the list of so far synthesized MAX phases, expectations about Zr_2AlC stability (at least compared to $ZrC + Zr_3Al_2$) have to be low since none of the Al neighbors (Si, Ga and Ge) forms a Zr_2AC MAX phase^{4,27–31}. Conversely some of Bi neighbors forms a Zr_2AC MAX phase ($A = Pb, Sn$). That and the lower formation enthalpy of Zr_2BiC compared to Zr_2AlC (Fig. 4) strongly suggests Bi presence is stabilizing the MAX structure. However, too much Bi (or too little Al) was predicted by DFT to render Bi much more covalent in Zr_2BiC than usually seen in MAX phases. This difference of Bi behavior in Zr_2BiC compared to $Zr_2(Al_{1-x}Bi_x)C$ ($0.25 \leq x \leq 0.75$) is therefore likely to be directly or indirectly responsible for the apparent non-stability of Zr_2BiC although $Zr_2(Al_{0.42}Bi_{0.58})C$ is experimentally stable.

In summary, the present study has considered the synthesis of $Zr_2(Al_{1-x}Bi_x)C$ MAX phases. It is determined here that $Zr_2(Al_{1-x}Bi_x)C$ and especially $Zr_2(Al_{0.42}Bi_{0.58})C$ forms in contrast to Zr_2BiC and Zr_2AlC that seemingly do not. DFT supports the experimental results as there is significant mixing enthalpy decrease when considering the $Zr_2(Al_{1-x}Bi_x)C$ MAX phase with respect to the end-members. This also demonstrates that an intermediate 211 MAX phase can form without the end members forming. If Zr_2AlC is most probably “simply” unstable or less stable than competing phases ($ZrC + Zr_3Al_2$), Zr_2BiC experimental non-stability may stem from an increase in Bi covalence strength for high Bi contents, as observed in DFT calculations. The inclusion of Bi is a significant extension of the MAX phase family and this should lead to further investigation of its material properties and technological applications. As an example, $Zr_2(Al_{0.42}Bi_{0.58})C$ may be a possible precursor for Zr_2C MXene synthesis.

Methods

Experimental methods. Zirconium dihydride (ZrH_2 , Alfa Aesar, – 325 mesh, >99.7%), bismuth (Alfa Aesar, – 325 mesh, >99.5%), aluminium (Alfa Aesar, – 325 mesh, >99.5%) and graphite (Sigma-Aldrich, – 500 mesh, >99.9%) were used as reactants. To limit as much as reasonably possible oxygen impurities, the reactants were kept and weighed in Nylon milling jars filled with 10 mm ZrO_2 balls in an Argon glove box. The jars were sealed and placed for 30 mins at 360 rpm in a rotary mill (Nanjing University Instrument Plant). The mixed powders were then transferred in the glove box, sealed in plastic bottles and kept in these bottles up until synthesis reaction. As is the custom for most MAX phase syntheses, stoichiometries were experimentally adjusted to 2/1.05/0.95 for Zr, Al + Bi and C, respectively. This is in order to compensate for the usual partial sublimation of the A element(s) and the possible partial uptake of carbon from the employed graphite crucibles and dies. Reactions were done by pressureless heating of the powders. Minutes before the thermal treatment, the sealed Ar-filled bottles were opened and poured in graphite crucibles (custom-made by Almath Crucibles Ltd., UK) which were then placed in a furnace under argon (FCT Systeme HP W/25/1, Rauenstein, Germany). Three different synthesis temperatures were tested: 1450 °C (1 h plateau), 1300 °C (10 h) and at 1150 °C (10 h). Heating and

cooling rates were set at $\sim 20^\circ\text{C}\cdot\text{min}^{-1}$. The obtained compounds were then analysed by XRD using a Bruker D2 Phaser SSD160 (Karlsruhe, Germany). Routine analyses consisted of 6 to $105^\circ 2\theta$ scans with a $0.03^\circ 2\theta$ step and $0.4\text{ sec}\cdot\text{step}^{-1}$. Crystalline phase determination was done with the help of Xpert High Score Plus software using ICDD (International Centre for Diffraction Data) database. As Zr_2BiC and Zr_2AlC are obviously not reported in the database Zr_2PbC and Zr_2SC were used as references for tentative matching. Similarly, the presence of higher order MAX phase ($n = 2$ or 3) was ruled out by comparison with simulated patterns using Crystal Maker and Crystal Diffract software. Refinement of unit cell parameters was done by full-pattern matching (Le Bail function) using the Fullprof Suite program³⁸. The powder obtained after 1300°C synthesis of $\text{Zr}_2(\text{Al}_{0.5}\text{Bi}_{0.5})\text{C}$ was manually milled in an agate mortar and underwent a $< 250\ \mu\text{m}$ sieving to be used for SPS sintering. This was done at Nanoforce lab., Queen Mary University of London, using a HP D/25/1 FCT System equipment and 30 mm graphite cylindrical mold jacketed with graphite paper. Sintering was done at 1300°C during 10 minutes, this temperature being reached in about 10 minutes. SEM imaging and EDX analyses were performed at 20 keV using a JEOL SEM 6400 equipped with an INCA detector (ultra-thin polymer window, Oxford Instruments, Oxford, UK).

Computational methods. DFT calculations were performed on the $\text{Zr}_2(\text{Al}_{1-x}\text{Bi}_x)\text{C}$ system using the VASP program. The GGA-PBE exchange correlation was used with pseudopotentials available in the library distributed with the VASP program³⁹ (using the highest valence electron version available). Calculations were carried out in a $4 \times 4 \times 1$ supercell (unit cell displayed in Fig. 1), containing 32 formula units (128 atomic sites). A $4 \times 4 \times 4$ γ -centered k-point grid was utilized for all calculations providing a spacing of $0.02\ \text{\AA}^{-1}$. A Methfessel-Paxton smearing method was used for all calculations with a smearing width of 0.15 eV. All calculations were performed under constant pressure, allowing all atomic positions, lattice parameters and angles to fully relax. The DOS of each system was modelled from the fully geometry optimized state.

Complete random mixing on the A sublattice was investigated by randomly populating Bi and Al species over the 32 available lattice sites. Seven different deviations in stoichiometry were investigated, namely: $x = 0.25, 0.33, 0.41, 0.50, 0.59, 0.66$ and 0.75 (in $\text{Zr}_2(\text{Al}_{1-x}\text{Bi}_x)\text{C}$). Ten random supercells of each stoichiometry were generated and relaxed using the method described. The standard deviation in energy was less than 0.02 eV/per $\text{Zr}_2(\text{Al}_{1-x}\text{Bi}_x)\text{C}$ unit.

Formation enthalpies H_{form} were calculated from the constituent elements (i.e. Zr metal, Al metal, Bi metal and C). The mixing enthalpy H_{mix} was subsequently calculated from these values, to highlight any preferred stoichiometry that forms as an intermediate composition (negative deviations of mixing enthalpies highlight a preferential system stoichiometry).

$$H_{\text{mix}} = H_{\text{form}}(\text{Zr}_2(\text{Al}_{1-x}\text{Bi}_x)\text{C}) - (1-x)H_{\text{form}}(\text{Zr}_2\text{AlC}) - xH_{\text{form}}(\text{Zr}_2\text{BiC}) \quad (1)$$

References

- Barsoum, M. W. & Radovic, M. Elastic and mechanical properties of the MAX Phases. *Ann. Rev. Mater. Res.* **41**, 195–227 (2011).
- Nowotny H. Strukturchemie einiger verbindungen der ubergangsmetalle mit den elementen C, Si, Ge, Sn. *Prog. Solid State Chem.* **2**, 27–70 (1970).
- Barsoum, M. W. & El-Raghy, T. Synthesis and characterization of a remarkable ceramic: Ti_3SiC_2 . *J. Am. Ceram. Soc.* **79**, 1953–1956 (1996).
- Barsoum, M. W., Yaroshuck, B. G. & Tyagi, S. Fabrication and characterization of M_2SnC ($\text{M} = \text{Ti, Zr, Hf}$ and Nb). *Scr. Met. Mater.* **37**, 1583–1591 (1997).
- Barsoum, M. W., Brodtkin, D. & El-Raghy, T. Layered machinable ceramics for high temperature applications. *Scr. Met. Mater.* **36**, 535–541 (1997).
- Naguib, M. *et al.* Two dimensional nanocrystals produced by exfoliation of Ti_3AlC_2 . *Adv. Mater.* **23**, 4248–4253 (2011).
- Naguib, M. *et al.* Two-dimensional transition metal carbides. *ACS Nano*. **6**, 1322–1331 (2012).
- Sun, Z. M. Progress in research and development on MAX phases: a family of layered ternary compounds, *Int. Mater. Rev.* **56**, 143–166 (2011).
- Hu, C., Zhang, H., Li, F., Huang, Q. & Bao, Y. New phases' discovery in MAX family. *Int. J. Refract. Met. Hard Mater.* **36**, 300–312 (2013).
- Naguib, M. *et al.* New solid solution MAX phases: $(\text{Ti}_{0.5}\text{V}_{0.5})_3\text{AlC}_2$, $(\text{Nb}_{0.5}\text{V}_{0.5})_2\text{AlC}$, $(\text{Nb}_{0.5}\text{V}_{0.5})_4\text{AlC}_3$ and $(\text{Nb}_{0.8}\text{Zr}_{0.2})_2\text{AlC}$. *Mater. Res. Lett.* **2**, 233–240 (2014).
- Horlait, D., Grasso, S., Al Nasiri, N., Burr, P. A. & Lee, W. E. Synthesis and high-temperature oxidation of MAX phases in the Cr-Ti-Al-C quaternary system. *J. Am. Ceram. Soc.* doi: 10.1111/jace.13962 (2015).
- Mockute, A. *et al.* Solid solubility and magnetism upon Mn incorporation in bulk Cr_2AlC and Cr_2GaC MAX phases. *Mater. Res. Lett.* **3**, 16–22 (2015).
- Nappe, J. C. *et al.* Damages induced by heavy ions in titanium silicon carbide: effects of nuclear and electronic interactions at room temperature. *J. Nucl. Mater.* **385**, 304–307 (2009).
- Tallman, D. J. *et al.* Effect of neutron irradiation on select MAX phases. *Acta Mater.* **85**, 132–143 (2015).
- Wang, J. & Zhou, Y. Recent progress in theoretical prediction, preparation, and characterization of layered ternary transition-metal carbides. *Annu. Rev. Mater. Res.* **39**, 415–443 (2009).
- He, L. F. *et al.* Isothermal oxidation of bulk $\text{Zr}_2\text{Al}_3\text{C}_4$ at 500 to 1000 $^\circ\text{C}$ in air. *J. Mater. Res.* **23**, 359–366 (2008).
- Music, D., Sun, Z., Ahuja, R. & Schneider, J. M. Electronic structure and shearing in nanolaminated ternary carbides. *Phys. Rev. B* **73**, 134117 (2006).
- Warner, J. A., Patil, S. K. R., Khare, S. V. & Masiulaniec, K. C. Ab initio calculations for properties of MAX phases Ti_2TlC , Zr_2TlC , and Hf_2TlC . *Appl. Phys. Lett.* **88**, 101911 (2006).
- Fang, C. M. *et al.* General trend of the mechanical properties of the ternary carbides M_3SiC_2 ($\text{M} = \text{transition metal}$). *Phys. Rev. B* **74**, 054106 (2006).
- He, X., Bai, Y., Zhu, C. & Barsoum, M. W. Polymorphism of newly discovered Ti_4GaC_3 : A first-principles study. *Acta Mater.* **59**, 5523–5533 (2011).
- Middleburgh, S. C., Lumpkin, G. R. & Riley, D. Accommodation, accumulation, and migration of defects in Ti_3SiC_2 and Ti_3AlC_2 MAX phases. *J. Am. Ceram. Soc.* **96**, 3196–3201 (2013).
- Istomin, P. V., Nadutkin, A. V., Ryabkov, Y. I. & Goldin, B. A. Preparation of Ti_3SiC_2 . *Inorg. Mater.* **42**, 250–255 (2006).
- Cover, M. F., Warschkow, O., Bilek, M. M. M. & McKenzie, D. R. A comprehensive survey of M_2AX phase elastic properties. *J. Phys.: Condens. Matter* **21**, 305403 (2009).

24. Dahlqvist, M., Alling, B. & Rosén, J. Stability trends of MAX phases from first principles. *Phys. Rev. B* **81**, 220102 (2010).
25. Keast, V. J. Harris, S. & Smith, D. K. Prediction of the stability of the $M_{n+1}AX_n$ phases from first principles. *Phys. Rev. B* **80**, 214113 (2009).
26. Bai, Y., He, X., Wang, R. & Zhu, C. An ab-initio study on compressibility of Al-containing MAX-phase carbides. *J. Appl. Phys.* **114**, 173709 (2013)
27. Opeka, M., Zaykoski, J., Talmy, I. & Causey, S. Synthesis and characterization of Zr_2SC ceramics, *Mater. Sci. Eng. A* **528**, 1994–2001 (2011).
28. El-Raghy, T., Chakraborty, S. & Barsoum, M. W. Synthesis and characterization of Hf_2PbC , Zr_2PbC and M_2SnC ($M=Ti, Hf, Nb$ or Zr) *J. Eur. Ceram. Soc.* **20**, 2619–2625 (2000).
29. Kulkarni, S. R., Phatak, N. A., Saxena, S. K., Fei, Y. & Hu, J. High pressure structural behavior and synthesis of Zr_2SC . *J. Phys.: Condens. Matter* **20**, 135211 (2008).
30. Gupta, S., Hoffman, E. N. & Barsoum, M. W. Synthesis and oxidation of Ti_2InC , Zr_2InC , $(Ti_{0.5}Zr_{0.5})_2InC$ and $(Ti_{0.5}Hf_{0.5})_2InC$ in air. *J. Alloys Compd.* **426**, 168–175 (2006).
31. Jeitschko, W., Nowotny, H. & Benesovsky F. Carbides of formula T_2MC . *J. Less-Comm. Met.* **7**, 133–138 (1964).
32. Barsoum, M. W. The $M_{n+1}AX_n$ phases: a new class of solids; thermodynamically stable nanolaminates. *Prog. Solid State Chem.* **28**, 201–281 (2000).
33. Aryal, S., Sakidja, R., Barsoum, M. W. & Ching, W. Y. A genomic approach to the stability, elastic, and electronic properties of the MAX phases. *Phys. Stat. Solidi B* **251**, 1480–1497 (2014).
34. Khazaei M., Arai, M., Sasaki, T., Estili M. & Sakka, Y. Trends in electronic structures and structural properties of MAX phases: a first-principles study on M_2AlC ($M = Sc, Ti, Cr, Zr, Nb, Mo, Hf, or Ta$), M_2AlN , and hypothetical M_2AlB phases. *J. Phys.: Condens. Matter* **26**, 505503 (2014).
35. Bouhemadou, A., Khenata, R. & Chegaar, M. Structural and elastic properties of Zr_2AlX and Ti_2AlX ($X = C$ and N) under pressure effect. *Eur. Phys. J. B* **56**, 209–215 (2007).
36. Yakoubi, A., Beldi, L., Bouhafs, B., Ferhat, M. & Ruterana, P. Full-relativistic calculation of electronic structure of Zr_2AlC and Zr_2AlN . *Solid State Comm.* **139**, 485–489 (2006).
37. Kang, D. B. Influence of different A elements on bonding and elastic properties of Zr_2AC ($A = Al, Si, P, S$): a theoretical investigation. *Bull. Korean Chem. Soc.* **34**, 609–614 (2013).
38. Roisnel, T. & Rodriguez-Carvajal, J. Winplotr: a windows tool for powder diffraction patterns analysis. *Mater. Sci. Forum* **118**, (2011).
39. Kresse, G. & Furthmuller, J. Efficient iterative schemes for ab initio total-energy calculations using a plane-wave basis set. *Phys. Rev. B* **54**, 11169 (1996).

Acknowledgements

Ben Milsom and Salvatore Grasso are acknowledged for their help in the access and use of Queen Mary University London equipment. A.C. is grateful for funding from the Lloyd's Register Foundation, a charitable foundation helping to protect life and property by supporting engineering-related education, public engagement and the application of research. D.H. thanks the EPSRC for funding through the XMat grant (EP/K008749/1). Calculations were undertaken with the assistance of resources provided at the NCI National Facility systems at the Australian National University through the National Computational Merit Allocation Scheme supported by the Australian Government. This work was also supported by the Multi-modal Australian ScienceS Imaging and Visualisation Environment (MASSIVE).

Author Contributions

D.H. performed the experiments and S.C.M performed the calculations. A.C. and W.E.L. helped analysing the results, contributed to the discussion and managed the funding of the work.

Additional Information

Competing financial interests: The authors declare no competing financial interests.

How to cite this article: Horlait, D. *et al.* Synthesis and DFT investigation of new bismuth-containing MAX phases. *Sci. Rep.* **6**, 18829; doi: 10.1038/srep18829 (2016).



This work is licensed under a Creative Commons Attribution 4.0 International License. The images or other third party material in this article are included in the article's Creative Commons license, unless indicated otherwise in the credit line; if the material is not included under the Creative Commons license, users will need to obtain permission from the license holder to reproduce the material. To view a copy of this license, visit <http://creativecommons.org/licenses/by/4.0/>